Joint Pathology Center
Veterinary Pathology Services

WEDNESDAY SLIDE CONFERENCE 2016-2017

C o n f e r e n c e 1

24 August 2016

CASE I: 48422 (JPC 4006379).

Signalment: 4-year-old male castrated sable ferret (*Mustela putorius furo*).

History: The ferret presented with a one-week history of ataxia. The owner noted a mass on the left neck. The ferret was eating but otherwise lethargic. Owners elected euthanasia due to worsening of clinical signs and the inoperable nature of the mass.

Gross Pathology: Within the subcutis and skeletal muscle of the neck just caudal to the skull, there is a large, firm, multinodular, smooth, white to tan, 5 x 3.5 x 1.5 cm mass extending to the left lateral and ventral aspect of the neck. The mass is adhered to the first cervical vertebra, extending caudally to the mid-cervical region and ventrally to the level of the trachea, but is not adhered to the trachea or esophagus. The central region of the mass is attenuated. After removal of the skull, evaluation of C1 reveals that the mass infiltrates into and effaces the left cranial articular fovea (articular facet of the atlas). After decalcification, further sectioning of the mass reveals that it extends into the vertebral canal and compresses the cervical spinal cord.

Cervical vertebrae, ferret. A large mass is present over the cranial cervical vertebrae. (Photo courtesy of: Animal Medical Center, 510 East 62nd St. New York, NY 10065 http://www.amcny.org/)

In the caudal aspect of the left cranial lung lobe, a 0.5 cm diameter firm, smooth, white nodule is observed. The spleen is diffusely congested and enlarged, and contained a 2 x 2 x 1.2 cm soft, smooth, red nodule. Two renal cortical cysts are observed in the right kidney, measuring approximately 0.4 cm each.

Laboratory results: N/A

Histopathologic Description: A de-calcified transverse section through the cervical vertebra, cervical spinal cord and

surrounding skeletal muscle is examined. Infiltrating into the epaxial musculature, cervical vertebral pedicle, articular processes and extending into the vertebral canal with compression of the adjacent cervical spinal cord is a multilobular, infiltrative, poorly demarcated neoplasm. Neoplastic lobules are separated by eosinophilic fibrovascular connective tissue. Lobules are comprised of large polygonal cells with distinct cell borders and abundant, amphophilic to clear, vacuolated cytoplasm (physaliferous cells) surrounded by variable amounts of amphophilic, mucinous stroma. Nuclei are round to oval and often peripheralized, with finely stippled chromatin and multiple nucleoli. There are zero mitotic figures in 10 high power (400x) fields. Multifocally in the center and at the periphery of lobules, scattered aggregates of cartilage and woven bone are interspersed within the physaliferous cells. Bony trabeculae contain osteocytes and are lined by osteoblasts. Chondrocytes lie within a lightly eosinophilic to amphophilic matrix or are occasionally entrapped within bone. Rare binucleate cells are found. Small aggregates of lymphocytes, plasma cells and macrophages are present at the periphery of the mass.

Cervical vertebra, ferret. This fixed specimen (likely proximal C-3 with dorsal spinous process at 10 o'clock) is unilaterally effaced by a multilobular mass which also compresses the spinal cord. (Photo courtesy of: Animal Medical Center, 510 East 62nd St. New York, NY 10065 http://www.amcny.org/)

Cervical vertebra (presumptive axis), ferret. The cervical vertebra is partially effaced by the chordoma, which compresses the spinal cord. (HE, 5X)

Vertebral bone has scalloped borders, with osteoclasts in Howship's lacunae. Fragmented woven bone (reactive bone) is interspersed with numerous plump osteoblasts and fibroblasts. Neoplastic compression of the cervical spinal cord results in shifting of the ventral medial fissure away from the mass. The white matter of the spinal cord exhibits mild, multifocal vacuolation in the dorsal, lateral and ventral funiculi, within which are few Gitter cells containing myelin degradation products. Scattered, multifocal swollen axons (spherocytes) are present in the ventral and lateral funiculi. Variation in neuronal cytoplasmic staining is present with no loss of Nissl substance (decalcification artifact, presumptive). Surrounding epaxial skeletal muscles, and more prominently, muscle adjacent to the dorsal spinous process undergoes degeneration and regeneration, manifesting as myocyte size variation, sarcoplasmic hypereosinophila and vacuolation, loss of striation, satellitosis, central nuclei, and nuclear rowing.

Contributor's Morphologic Diagnoses: 1. Cervical spine: Chordoma, with local

infiltration of skeletal muscle, vertebral bone and vertebral canal.
2. Cervical spinal cord: Focal compression with midline shift, mild, moderate Wallerian degeneration and spheroid formation.
3. Cervical skeletal muscles: Multifocal myodegeneration and regeneration.
4. Lung (caudal aspect left cranial lung lobe, not submitted): Multifocal chordoma metastasis.

Contributor's Comment: Chordomas are the 5th most common tumor in domestic ferrets, and the most common musculoskeletal tumor.[1,11] Chordomas are slow growing, locally aggressive neoplasms derived from remnant fetal notochord [1,4,6-12,14] believed to originate from the primitive mesoderm.[1,2] The notochord persists between the vertebrae and expands to form the nucleus pulposus of intervertebral disks in some animals (visible in the section).[1,5,8,9] Cell rests of residual notochord remain outside of the intervertebral disks in an estimated 2% of humans, and chordomas are thought to arise from these cell rests.[1,4,8,9] Histologically, ferret chordomas are characterized by lobules of physaliferous cells surrounding cartilage with a central core of bone and cartilage. [1,4,6-12,14] Notochord-induced differentiation of bone and cartilage within the neoplasm is one hypothesis for the bone and cartilage formation within these neoplasms.[4]

Chordomas can occur anywhere along the axial skeleton. In the ferret, common sites include the tail tip (most common site), cervical vertebral column (second most common site**),** thoracic vertebral column, and the coccygeal region.[1,4,6-12,14] The sacrococcygeal and spheno-occipital regions are the most common sites of chordoma occurrence in humans, with the remainder

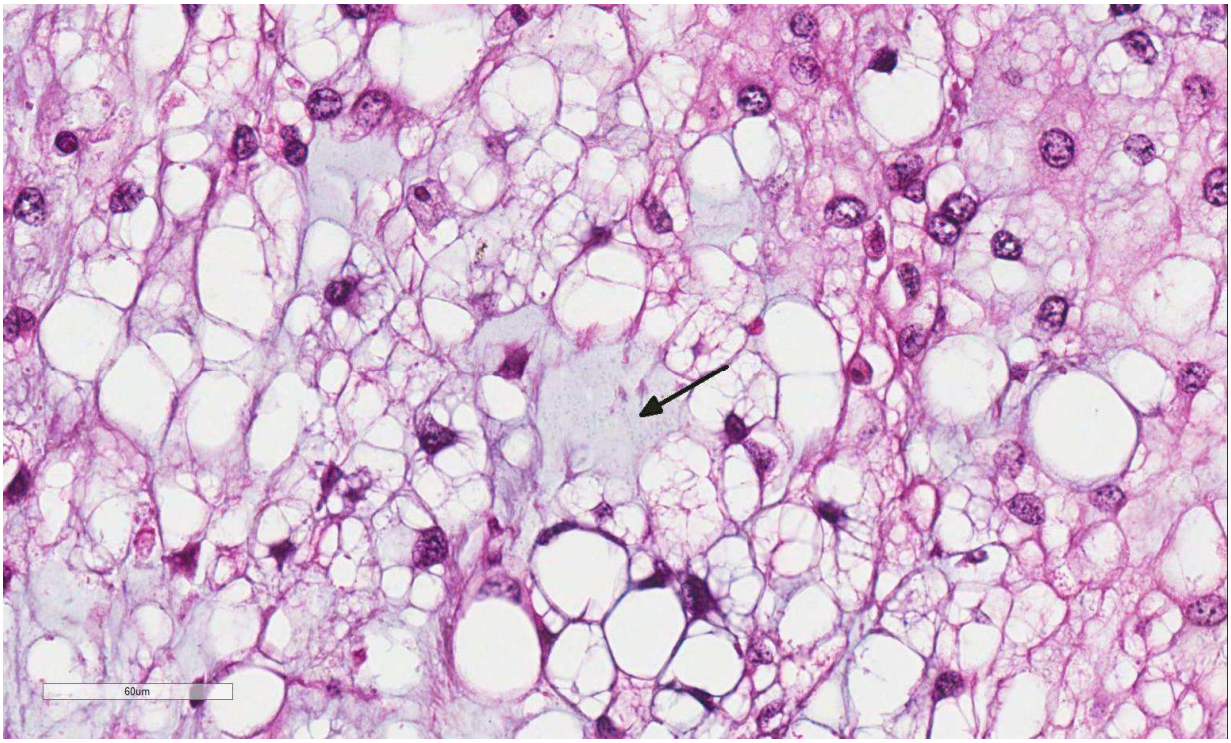

Cervical vertebra (presumptive axis), ferret. The neoplasm is composed of polygonal cells with large clear vacuoles which often peripheralize the nucleus (physaliferous cells) separated by moderate amounts of blue mucinous matrix (arrow). (HE, 400X)

found in the vertebral axis.[4,14] Up to 30% of human chordomas are reported to metastasize, typically during the phase of recurrent disease, with common sites of metastasis reported to be bone, lung, lymph node, skin and liver.[1,4,14] Rare cases of local and distant skin metastases have been reported in the ferret.[1,4,14] Vascular invasion was equivocal in the submitted section, however, was observed rarely in other sections of the mass and pulmonary metastases were present. One study evaluated cell proliferation indices in 5 ferret chordomas, and found that they were not predictive of metastatic potential.[8]

In humans, there are 3 recognized subtypes of chordoma: classic chordoma, chondroid chordoma, and chordoma with malignant spindle cell component (dedifferentiated). It has been suggested that ferret chordomas may act as an animal model for the chondroid subtype of human chordoma.[4,14] Differentiation between classic and chondroid subtypes in humans is significant, as chondroid chordomas are associated with a survival rate 3 times greater than that of classic chordomas.[1,8] Although the chondroid component was not prominent in the submitted section, it was more frequently observed in other sections of the mass.

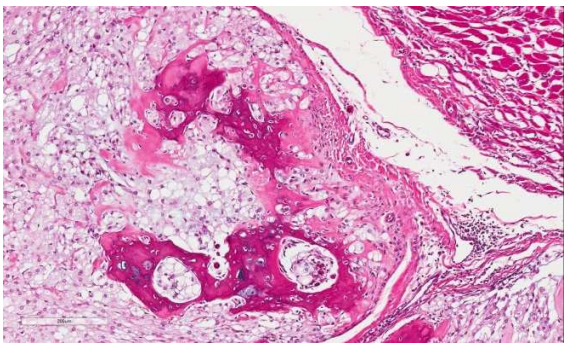

Cervical vertebra (presumptive axis), ferret. Multifocally, several lobules of the neoplasm contain foci of mineralizing woven bone. (HE, 200X)

Immunohistochemical analysis of chordomas in the ferret typically show dual expression of cytokeratin and vimentin, with variable expression of S-100 protein and neuron specific enolase (NSE).[1,4,6-12,14] In one study of chordomas in 20 ferrets, 75% were positive for S-100 and 85% were positive for NSE.[4] The S-100 positivity is thought to be due to glycosaminoglycan content within the stroma, and NSE is expressed in cells with high metabolic activity.[1,4]

JPC Diagnosis: Cervical vertebra (axis): Chordoma.

Conference Comment: This case nicely characterizes an example of a common neoplasm in the axial skeleton of a ferret. The contributor provides an excellent histologic description, including the ancillary findings of degeneration of the spinal cord, peripheral nerves, and adjacent skeletal muscle as a result of compression from this infiltrative neoplasm.

Aside from humans and ferrets, chordomas have been rarely reported in the axial skeleton of Fischer 344 rats[11], mice[13], dogs[6,9], and cats[2]. In addition, 24 cases of spontaneous primary intestinal chordomas as well as nine spontaneous vertebral chordomas, were recently reported in the aged laboratory zebrafish[3]. In dogs, chordomas have been reported in the brain, spinal cord, and skin[6]. Of the three reported cases of feline chordoma, one was initially diagnosed as chronic granulomatous inflammation due to the interpretation of the characteristic physaliferous cells as atypical, foamy macrophages; it was subsequently dis-covered to be an example of a classic chordoma-like subtype, which then metastasized to multiple lymph nodes[2].

In all species, chordomas tend to be slow growing and locally invasive.[1-14] Typically, distant metastasis is associated with the classic chordoma and dedifferentiated spindle cell subtypes in humans, rather than the chondroid type which forms islands of cartilage and bone most commonly in the ferret and mink.[1,4,8,10,14] In a large study of Fischer 344 rats there was an exceptionally high 75% incidence of pulmonary metastasis in animals diagnosed with chordomas.[11] The histomorphology of chordomas in the Fischer rat is similar to the classic type in humans, which may explain the more aggressive biologic behavior in these rodents as compared to other animals.[11] Prior to this case, visceral metastasis had not yet been reported in the ferret. However, the contributor recently published this case report, to include pulmonary metastasis via hematogenous spread; this is the first known case of visceral metastasis in the ferret[5]. The authors hypothesized that the metastatic potential in ferrets may increase over time, highlighting the importance of prompt surgical excision. Most cases of ferret chordomas occur at the tail tip making complete surgical excision relatively simple.[1,4,5,14] Chordomas in other locations, such as this case, are substantially more difficult to excise.[5]

Chordomas in ferrets may histologically resemble chondrosarcomas due to the cartilaginous component. Conference participants briefly discussed immunohistochemistry as a method by which to differentiate chordoma from chondrosarcoma. As mentioned by the contributor, chordomas consistently demonstrate dual immunopositivity for vimentin and cytokeratin, while chon-drosarcomas are immunonegative for cytokeratin. Chordomas are also typically positive for S-100 and neuron-specific enolase (NSE); the S-100 and NSE positivity does not suggest neural crest origin, however.[10,12] Other neoplasms of interest that typically express both vimentin and cytokeratin include: mesothelioma, synovial sarcoma, meningioma, renal cell carcinoma, adrenal carcinoma, and endometrial sarcoma.[12]

Contributing Institution: The Animal Medical Center
Department of Pathology
510 East 62nd St. New York, NY 10065
http://www.amcny.org/

References:

1. Camus MS Rech RR, Choy FS, Fiorello CV, Howerth EW. Pathology in practice, chordoma on the tip of the tail of a ferret. *J Am Vet Med Assoc*. 2003;235(8):949-51.
2. Carpenter JL, Stein BS, King NW Jr, Dayal YD, Moore FM. Chordoma in a cat. *J Am Vet Med Assoc.* 1990;197:240-242.
3. Cooper T, Murray K, et al. Primary intestinal and vertebral chordomas in laboratory zebrafish (*Danio rerio*). *Vet Pathol*. 2015;52(2):388-392.
4. Dunn DG, Harris RK, Meis JM, Sweet DE. A histomorphologic and immune-ohistochemical study of chordoma in twenty ferrets (*Mustela putorius furo*). *Vet Pathol*. 1991;28:467-473.
5. Frohlich J, Donovan T. Cervical chordomas in a domestic ferret (Mustela putorius furo) with pulmonary metastasis. *J Vet Diagn Invest*. 2015;27(5)656-659.
6. Gruber A, Kneissi S, Vidoni B, Url A. Cervical spinal chordoma with chondromatous component in an dog. *Vet Pathol.* 2008;45(5):650653.
7. Koestner A, Bilzer T, Fatzer R, Schulman FY, Summers BA, Van Winkle TJ. Chordoma. In: *Histological Classification of Tumors of the Nervous System of Domestic Animals*, 2nd series, vol. V, pp. 36. Armed Forces Institute of Pathology, Washington, D.C., 1999.

8. Munday JS Brown CA, Richey LJ. Suspected metastatic coccygeal chordoma in a ferret (*Mustela putorius furo*). *J Vet Diagn Invest.* 2004;16(5):454-458.
9. Munday JS, Brown CA, Weiss R. Coccygeal chordoma in a dog. *J Vet Diagn Invest.* 2003;15(3):285-288.
10. Pye GW, Bennett RA, Roberts GD, Terrell SP. Thoracic vertebral chordoma in a domestic ferret (*Mustela putorius furo*). *J Zoo Wildl Med* 2000;31(1):107-111.
11. Stefanski SA, Elwell MR, Mitsumori K, Yoshitomi K, Dittrich K, Giles HD. Chordomas in Fischer 344 rats. *Vet Pathol.* 1988;25(1):42-47.
12. Takeshi Y, Tetsuo O, et al. Histochemical and immunohistochemical characterization of chordoma in ferrets. *J Vet Med Sci*. 2015;77(4):467-473.
13. Taylor, K, Garner M, et al. Chordomas at high prevalence in the captive population of the endangered Perdido Key Beach mouse (*Peromyscus polinotus trissyllepsis*). *Vet Pathol*. 2016;53(1):163-169.
14. Williams BH, Eighmy JJ, Berbert MH, Dunn DG. Cervical chordoma in two ferrets (*Mustela putorius furo*). *Vet Pathol*. 1993;30:204-206.

CASE II: 48422 (JPC 4006379).

Signalment: 16 year old, female, domestic shorthair, *Felis catus*.

History: The cat had decreased appetite and weight loss. It was icteric with a temperature of 38°C. The heart rate was 220 beats/min and the respiration rate was 92 breaths/min. Lymph nodes were unremarkable by palpation. Ultrasound of the abdomen showed moderate amounts of fluid, and a liver with rounded edges and a marbled parenchyma with reduced number of visible hepatic- and portal veins. Lymph nodes in the cranial abdomen, near the spleen and pancreas were enlarged and hypoechoic.

Gross Pathology: The cat was thin and icteric. The abdominal cavity contained 50 ml clear yellow fluid with a few floccules. The liver was slightly enlarged with rounded edges and lighter in color than normal with a lobular pattern and a decreased texture. Multifocally scattered, light gray, soft nodules, 0.5-5.0 mm in diameter were present in the hepatic parenchyma. The mesenteric lymph node was enlarged, light yellow-gray, moderately firm, and measured 4.0x1.5x1.5 cm. The pancreas was macroscopically normal.

Laboratory results: Clinical pathology: AST: 193 U/L (ref: 0-60), ALT: 258 U/L (ref: 0-75), AP: 339 U/L (ref: 0-40), amylase: 880 U/L (ref: 0-800), total protein: 56 g/L (ref: 60-82), albumin: 21 g/L (ref: 25-39), bile acids: 392 µmol/L (ref: 0-5), total bilirubin: 215 µmol/L (ref: 0-4), WBC: 4.2 x 10e9/L (ref: 5.5-17), lymphocytes: 0.6 x 10e9/L (ref: 1.5-7.0), platelets: 30 x 10e9/L (ref: 180-400).

Immunohistochemical staining of mesenteric lymph node and liver showed immunoreactivity with rabbit anti-human CD3 (DakoCytomation, A 0452) and confirmed that the infiltrating cells were T lymphocytes.

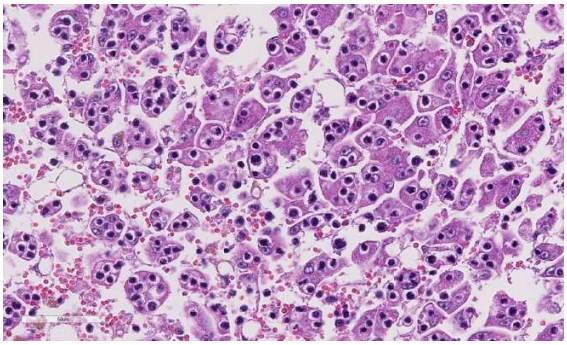

Liver, cat. Hepatic cords are diffusely dissociated and hepatocytes contain multiple lymphocytes within their cytoplasm. Intrahepatocytic lymphocytes are surrounded by a clear vacuole. (HE, 400X)

Histopathologic Description: In the liver, there are multifocal to confluent, randomly spaced areas with numerous infiltrating small lymphoid cells. The cells are located both in the sinusoids and appear to be located within the cytoplasm of hepatocytes. Some of the cells are also located close to or in invaginations of the hepatocellular membrane. The cells are small, with a narrow rim of eosinophilic cytoplasm. They have a small, densely stained round to irregular nucleus with indistinct nucleolus. There is little degree of anisocytosis and anisokaryosis. There is <1 mitotic figure per 10 HPF. The lymphoid cells present within the hepatocellular cytoplasm are surrounded by a clear halo. There is severe dissociation of hepatocytes, seen as single rounded large hepatocytes with up to 8 lymphoid cells within the cytoplasm. In areas with few lymphoid cells, there are moderate vacuolation of hepatocytes with variably sized clear vacuoles.

Contributor's Morphologic Diagnoses: Liver: malignant lymphoma with emperipolesis of lymphocytes and severe dissociation of hepatocytes

Contributor's Comment: Feline lymphoma commonly occurs as thymic, alimentary multicentric and cutaneous syndromes.[8] This cat had involvement of the mesenteric lymph node and liver. It is indicated that Feline leukemia virus (FeLV) positive cats are associated with the mediastinal and multicentric form of lymphoma and that the thymic and alimentary forms predominate in FeLV negative cats.[2,8] The FeLV status of this cat was not known.

Hepatic lesions morphologically identical to those in this cat, has been reported earlier in two cats diagnosed with lymphoblastic lymphosarcoma.[3]Although emperipolesis is the phenomenon of viable cells entering the cytoplasm of other cells without damage to either host cell or the engulfed cells,[3] the clinical pathology of this cat, similar to the cats presented by Ossent et al,[5] indicates severe hepatic failure. In addition, histology of the liver shows extensive hepatocellular dissociation.

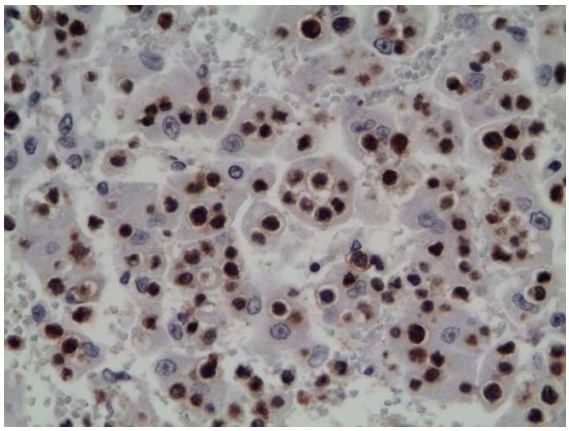

Liver, cat. Intrahepatocytic lymphocytes stain strongly positive with anti-CD-3 immunohistochemical stain. (anti-CD3, 400X) (Photo courtesy of: Norwegian School of Veterinary Science, Institute of Basic Sciences and Aquatic Medicine, PO box 8146 Dep, 0033 Oslo Norway. http://www.veths.no/Venstremeny/English/)

JPC Diagnosis: 1. Liver: T-cell lymphoma, hepatocytotropic.
2. Liver: Regeneration, micronodular, multifocal, mild.

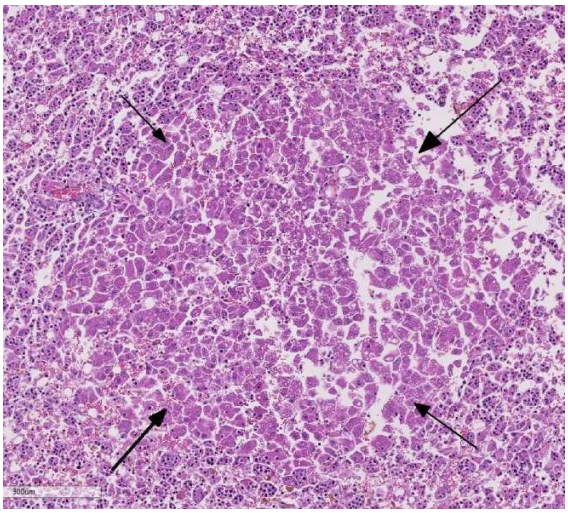

Liver, cat. Scattered throughout the section are rare nodules of proliferating hepatocytes which contain few intrahepatocytic lymphocytes (arrows). The mild lipidosis seen diffusely through the section is best demonstrated here. (HE, 400X)

Conference Comment: This case generated discussion amongst the conference participants regarding the use of the term emperipolesis. As mentioned by the contributor, emperipolesis is an uncommon biological process, in which a cell penetrates the cytoplasm of another living cell. [1,4,6,7] Unlike phagocytosis where the engulfed cell is killed by lysosomal enzymes of the macrophage, the engulfed cell exists as a viable cell within another.[7] The pathogenesis and significance of this phenomenon is currently unknown.[1] Emperipolesis has been rarely reported in the human literature associated with autoimmune hemolytic anemia, multiple myeloma, leukemia, and malignant lymphoma.[1] In this case, there is clear evidence of hepatocellular injury and cholestasis supported by the animal's clinical icterus along with severe serum biochemistry abnormalities. Clinicopathologic serum elevations in AST and ALT, as well as hypoalbuminemia and hypoproteinemia support hepatocellular injury in addition to hepatocellular swelling, lipofuscin deposition, and hepatic lipidosis. Cholestasis is confirmed by severe elevations in bile acids, total bilirubin, and elevated ALP.

Given the degree of hepatocellular injury and cholestasis, conference participants unanimously preferred the term hepatocytotropism over emperipolesis as a more representative term for the infiltrating T-cell lymphocytes in this case. This terminology was recently proposed as an alternative to emperipolesis in similar cases malignant lymphoma in the dog with distinct tropism for hepatocytes.[4] Transmission electron microscopy in the dog as well as the previously reported cases in cats, showed lymphocytes within invaginations of the hepatocyte cell membrane rather than within the cytoplasm, as required for emperipolesis.[4,6,7] In addition, hepatocytotropism is more analogous to the epitheliotropism present in cutaneous and intestinal T-cell lymphoma in the dog and cat.[4]

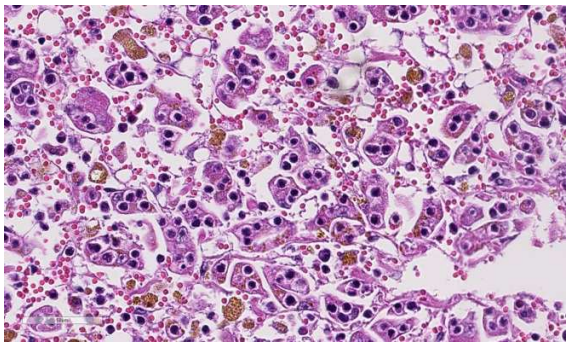

Liver, cat. In areas of marked hepatic cord dissociation, Kupffer cells contain abundant granular brown pigment, which likely represents a combination of iron (confirmed with Perl's stain), bile pigment, and lipofuscin from hepatocellular damage. (HE, 400X)

Several conference participants also commented on the degree of hepatic cord discohesion with dislocation of hepatic plates and diffuse loss of normal architecture in this case. Some speculated this to be partially due to moderate autolysis of the tissue. There was further discussion and

some speculation that hepatic discohesion could be due to a defect in β-catenin through the Wnt signaling pathway, common in hepatic neoplasms.[9] This pathway has a major role in cell adhesion to the basement membrane and cell polarity in the liver and gastrointestinal tract. In addition, β-catenin binding to E-cadherin is responsible for maintaining intercellular adhesion.[5] Normally, after acute hepatocellular insult, the liver is stimulated to regenerate via the Wnt pathway. The Wnt receptor signals through cell surface receptor, frizzled (FRZ), to deactivate the destruction complex, APC. The tumor suppressor APC normally binds to and destroys β-catenin.[5] With the APC deactivated, β-catenin signaling drives the expression of target genes that are critical for cell cycle progression and contribute to initiation of the regeneration process.[5,9] Even in the multifocal microregenerative nodules without hepatocytotropic lymphocytes, there is hepatic cord discohesion. Regardless of the pathogenesis, the disassociation of the hepatic cords likely disrupts bile canalicular transport and secretion of bilirubin leading to severe hepatic cholestasis and icterus in this case.[6]

Contributing Institution: Norwegian School of Veterinary Science
Institute of Basic Sciences and Aquatic Medicine
Oslo, Norway
http://www.veths.no/Venstremeny/English/

References:

1. Amita K, Shankar S, et al. Emeripolesis in a case of adult T cell lymphoblastic lymphoma (mediastinal type)-detected at FNAC and imprint cytology. *Online J Health Allied Scs.* 2011;10:11.
2. Fry, M, McGavin M. Bone marrow, blood cells, and the lymphatic system. In: Zachary JF, McGavin MD, eds. *Pathologic Basis of Veterinary Disease.* 5th ed. St. Louis, MO: Elsevier; 2012:698-705.
3. Humble JG, Jayne WHW, Pulvertaft RJV: Biological interaction between lymphocytes and other cells. *Br J Heamatol* 1956;2:283-294.
4. Keller S, Vernau W, et al. Hepatosplenic and hepatocytotropic T-cell lymphoma: two distinct types of lymphoma in dogs. *Vet Pathol*. 2012;50:281-290.
5. Kumar V, Abbas A, Aster J. Neoplasia. In: Kumar V, Abbas A, Aster J, eds. *Robbins and Cotran Pathologic Basis of Disease*. 9th ed. Philadelphia, PA; Saunders Elsevier; 2015: 296-297.
6. Ossent P, Stöckli RM, Pospischil A: Emperipolesis of lymphoid cells in feline hepatocytes. *Vet Pathol*. 1989;26:279-280.
7. Suzuki M, Kanae Y, et al. Emperipolesis-like invasion of neoplastic lymphocytes into hepatocytes in feline T-cell lymphoma. *J Comp Path*. 2011;144:312-316.
8. Valli V, Kiupel M, Bienzle D. Hematopoietic system. In: *Jubb, Kennedy, and Palmer's Pathology of Domestic Animals*, ed. Maxie MG, 4th ed., Vol. 3. Saunders Elsevier, Philadelphia, PA, 2016:103-104.
9. Wang E, Yeh S. et al. Depletion of β-catenin from mature hepatocytes of mice promotes expansion of hepatic progenitor cells and tumor development. *PNAS*. 2011;108:18384-18389.

CASE III: M (JPC 4035590).

Signalment: 16-week-old female and male mink kits, *Mustela vison*

History: Kits were vaccinated subcutaneously at 6 weeks of age with 3 portions of the 4-way combination vaccine including inactivated mink enteritis virus, *Clostridium botulinum* Type C bacterin-toxoid and inactivated *Pseudomonas*

aeruginosa bacterin. Kits were vaccinated at approximately 10-12 weeks of age with the modified- live canine distemper virus portion of the 4-way combination vaccine via aerosol spray.

Lung, mink. At subgross magnification, the section of lung is markedly congested. (HE, 5X)

Approximately 10 days later, mortality started with 5- 10 dead kits per day. Mortality was concentrated in 2 of 8 barns and the mahogany mink were primarily affected. Affected mink kits had "wet heads" and were screaming, seizuring before dying. This producer mixes his own feed on farm and in the last week, had a feed change to fish, chicken and processed meats. Only the chicken is fresh daily, the other protein sources are frozen. As of a week ago, antibiotics (CSP 250) were mixed in the feed. The older mink are fine.

Gross Pathology: Four mink kits were submitted for postmortem examination. They were in good body condition with ample internal and external fat stores. They were mildly to moderately dehydrated. The lungs were diffusely mottled purple/red and were edematous. The tracheal lumina did not contain fluid or exudate. Stomachs were generally either empty or contained brown flecked mucus or brown fluid. The small intestines were generally empty and only a small amount of gold brown mucoid to pasty material was in the rectum. Livers were red tinged with yellow. The spleens were small.

Laboratory results: Negative for Aleutian disease by CIE testing. Multiple tissues including lung, spleen, liver, adrenal gland and brain had positive immunohistochemical (IHC) staining for canine distemper virus (CDV).

Histopathologic Description: The lung is markedly congested with alveoli containing eosinophilic edema fluid, small amounts of fibrin and red blood cells. Multifocally, small to moderate numbers of macrophages with abundant often foamy cytoplasm, less frequently multinucleated cells and infrequent neutrophils are also collecting in alveolar spaces. Bronchial lumina contain eosinophilic edema fluid, small numbers of red blood cells, macrophages, multinucleate cells, neutrophils and degenerate cells. Many of the bronchi and nearby vessels are rimmed by one to two cell thick lymphohistiocytic cuffs. Numerous large eosinophilic spherical to rectangular inclusions morphologically compatible with viral inclusions are present within the cytoplasm of normal and proliferative bronchial and bronchiolar epithelium and occasionally within macrophages or multinucleated cells. Strong positive staining for CDV is present within bronchiolar epithelium and alveolar macrophages on immunohistochemistry.

Contributor's Morphologic Diagnoses: 1. Marked pulmonary congestion and moderate pulmonary edema.
2. Proliferative bronchitis, bronchiolitis and multifocal histiocytic pneumonia with eosinophilic intracytoplasmic inclusions.
3. Very mild acute suppurative bronchitis, bronchiolitis and pneumonia

Contributor's Comment: The host range of canine morbillivirus (canine distemper virus,

CDV) is broad and species in all families in the order Carnivora, including *Canidae*, *Mustelidae*, *Procyonidae*, *Hyaenidae*, *Ursidae* , *Viverridae* and *Felidae* are considered susceptible.[9] Canine distemper virus causes multisystemic disease in farmed mink[4] with juvenile mink being most susceptible with a mortality rate of 90% as compared to a more variable rate of 20-90% in adult mink.[9] Outbreaks of CDV infection on commercial mink farms have been associated with infected raccoons (*Procyon lotor*) and striped skunks (*Mephitis mephitis*) found on the farm premises[4]. The transmission of the virus is mainly by aerosol or through direct contact with oral, nasal or conjunctival fluid as the canine distemper virus does not survive long in the environment and it can be rapidly in-activated by ultraviolet light, drying, heat and common disinfectants. However, it is possible for the gloves used for handling infected mink to act as fomites and transmit sufficient virus to infect susceptible mink for a short period of time.[2]

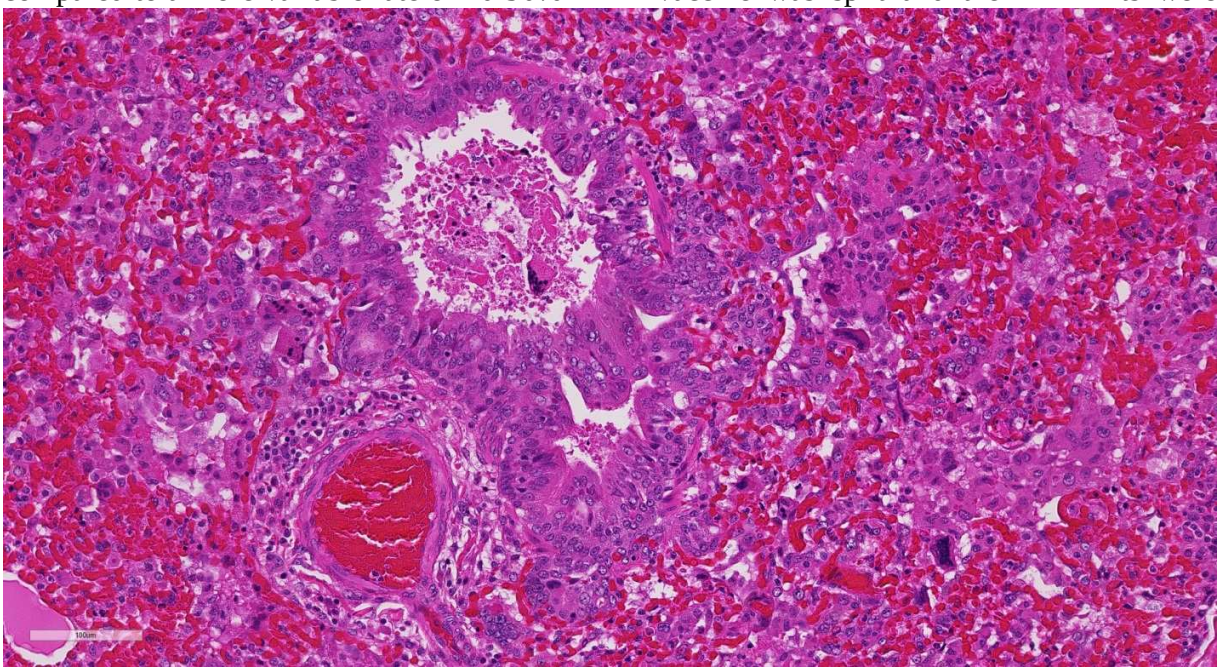

Lung, mink. There is marked hyperplasia of bronchiolar epithelium which extends into the surrounding alveoli. Viral syncytia may be seen in lumen of the affected airway as well as within macrophages in surrounding alveoli. (HE, 5X)

Routine vaccination of kits via subcutaneous injection using a multivalent vaccine including canine distemper virus is typically carried out after weaning.[4] Some producers will also revaccinate the mature females and males being retained for breeding at this time (J Mitchell, personal communication). On this farm, the 4-way combination vaccine was split and the mink kits were immunized by subcutaneous injection for mink enteritis virus, *Clostridium botulinum* Type C and *Pseudomonas aeruginosa* at 6 weeks of age. Four to six weeks later, the kits were given the canine distemper virus portion of the vaccine by aerosol spray, however, as the vaccine is meant to be given by subcutaneous injection it is likely the mink kits were not sufficiently immunized against canine distemper virus and subsequently developed clinical disease.

At necropsy, the most consistent lesions were identified in the lungs with pro-liferative bronchitis and bronchiolitis and variable numbers of large rectangular

eosinophilic intracytoplasmic inclusions identified in bronchial and bronchiolar epithelium. Low numbers of multinucleated cells in alveoli occasionally also contain intracytoplasmic inclusions. Small accumulations of neutrophils were aggregating in small airways and secondary bacterial bronchopneumonia is reported to commonly occur.[4] The diagnosis of CDV in these individuals was confirmed with IHC.

In experimental infections with the virus given by injection, young mink are reported to develop reddening of the skin progressing to dermatitis, conjunctivitis and nasal discharge, but dyspnea is uncommon.[4] However, histologically, pulmonary lesions are common and the intracytoplasmic and intranuclear viral inclusions are most often present in the respiratory or bladder epithelium.[4] Viral inclusions are not identified in the transitional epithelium of the bladder in this case, despite the tremendous numbers visible in the lung tissues.

JPC Diagnosis: Lung: Bronchiolar epithelial hyperplasia, marked, with mild histiocytic bronchiolitis, and epithelial and histiocytic intracytoplasmic viral inclusion bodies.

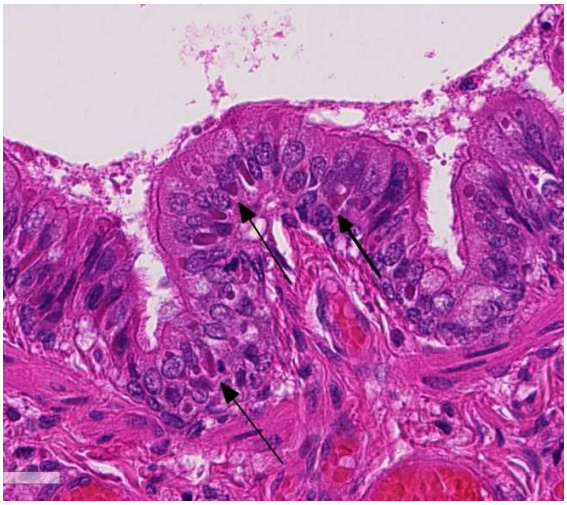

Lung, mink. Bronchiolar epithelium contains one or multiple 2-4um irregularly round intracytoplasmic viral inclusions. (HE, 320X)

Conference Comment: Canine distemper virus (CDV) is an enveloped, single stranded RNA (ssRNA) virus of the genus *Morbillivirus* in the *Paramyxoviridae* family[1-8]. *Morbilliviruses* are highly contagious pathogens that are responsible for some of the most devastating diseases that affect mammals worldwide. Other members of this genus include measles virus, peste des petits ruminants virus, rinderpest virus, phocine distemper virus, and dolphin morbillivirus.[6] CDV is one of the most important and ubiquitous infectious diseases of wild and domestic predators with high morbidity and mortality in imm-unologically naïve populations.[5] As men-tioned by the contributor, mustelids (i.e. ferrets, minks, and badgers) are particularly sensitive to the virus with mortality up to 100% in non-vaccinated ferrets.[5]

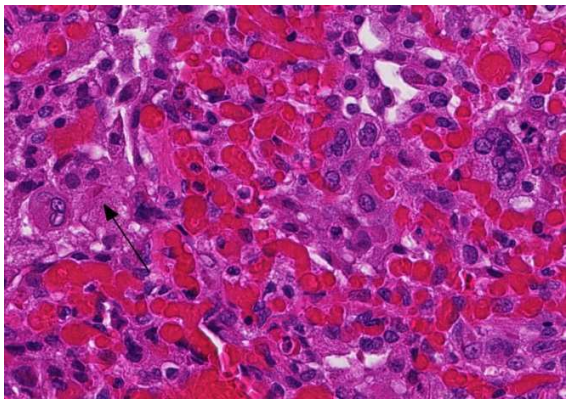

Lung, mink. Alveoli contain numerous macrophages which occasionally contain intracytoplasmic viral inclusions (arrow). A multinucleated viral syncytium is present at right. (HE, 400X)

Like all paramyxoviruses, CDV contains six structural proteins: nucleocapsid (N), phospho (P), large (L), matrix (M), hemagglutinin (H), and fusion (F) protein. The viral envelope contains *H*, used for attachment to the host cell receptor, and *F*, required for entry and syncytia formation. In

this case, syncytial cells are occasionally present within bronchioles and alveoli.[1,6]

CDV is typically transmitted via inhalation of infected aerosols.[3,4] The virus enters macrophages, lymphocytes, and dendritic cells via the signaling lymphocyte activation molecule (SLAM) receptor binding to H viral protein within the first day of infection.[1,6] The virus spreads to local lymph nodes and other lymphoid organs within two to five days post infection. Primary viral replication in the lymphoid tissues leads to severe immunosuppression and viremia. About eight to ten days post-infection, CDV disseminates to several epithelial tissues (respiratory, intestinal, and urinary) and the central nervous system. The virus uses epithelial cell receptor nectin-4 to gain entry into epithelial cells.[1,4,6]

Unfortunately, in this case, the conference participants had difficulty assessing the alveolar septal changes due to poor insufflation of the lung. However, conference participants easily identified numerous intracytoplasmic viral inclusions within histiocytes and the markedly hyperplastic bronchiolar epithelium. In addition, some recognized rare intranuclear inclusions. CDV is unique because it causes both intranuclear and intracytoplasmic inclusions.[3,7,8] Given that CDV is an ssRNA virus that requires RNA-dependent RNA polymerase complex present only in the cytosol to replicate, the presence of intranuclear inclusions is initially confounding.[7] However, CDV infection induces the cellular stress response which causes elevated expression of heat shock proteins. These proteins translocate viral nucleocapsid (N) proteins from the cytoplasm into the nucleus as part of the normal host cell response to cellular stress. Under normal circumstances, the N protein would be too large to pass through nuclear pores.[7] N proteins form the basis for nuclear body formation, and propagation of viral nucleocapsids. These particles eventually partially, or completely fill the nucleus resulting the in the formation of the intranuclear inclusion body visible by light microscopy.[7,8]

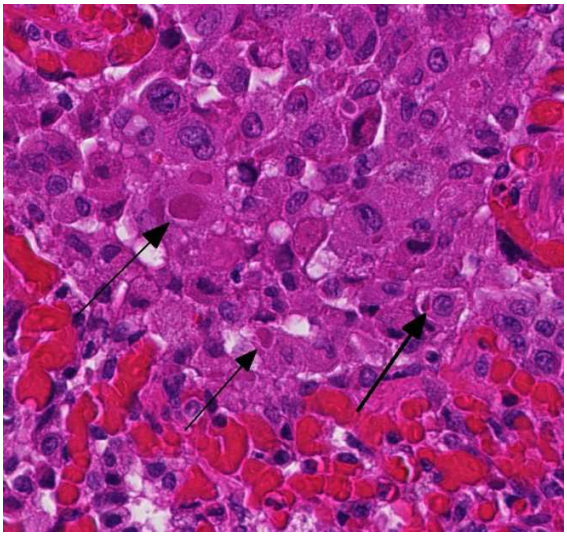

Lung, mink. In this field, numerous alveolar macrophages contain variably-sized viral inclusions (arrows). (HE, 400X)

The contributor mentions the wide range of species now infected by CDV and related viruses. Additionally, lethal outbreaks in rhesus and cynomolgus macaques originating in China have been documented within the last decade.

Contributing Institution: Animal Health Laboratory
University of Guelph, Guelph, Ontario, Canada
http://ahl.uoguelph.ca

References:

1. Beineke A, Baumgartner W, Wohlsein P. Cross species transmission of canine

distemper virus-an update. One Health. 2015; 1:49-59.
2. Budd J. Distemper. In: Infectious diseases of wild mammals. 1st ed. Ames, IA: Iowa State Press; 1970:36-49.
3. Caswell J, Williams K. Respiratory system. In: Maxie MG, ed. Jubb, Kennedy, and Palmer's Pathology of Domestic Animals. Vol 2. 6th ed. Philadelphia, PA: Elsevier Saunders; 2016: 574-575.
4. Hunter DB. Respiratory System of Mink. In: Hunter B, Lemieux N, eds. Mink: Biology, Health and Disease. Guelph, Ontario: Graphic and Print Services, University of Guelph; 1996:13-1 – 13-15.
5. Kuipel M, Perpinan D. Viral Diseases in Ferrets. In: Biology and Diseases of the Ferret. 3rd ed. Ames, IA: Wiley Blackwell; 2014:439-450.
6. Noyce R, Depeut S, Richardson C. Dog nectin-4 is an epithelial cell recepotor for canine distemper virus that facilitates virus entry and syncytia formation. Virology. 2013;436:210-220.
7. Oglesbee M. Intranuclear inclusions in paramyxovirus-induced encephalitis: evidence for altered nuclear body differentiation. Acta Neuropathol. 1992;84:407-415.
8. Oglesbee M, Krakowa S. Cellular stress response induces selective intranuclear trafficking and accumulation of morbillivirus major core protein. Lab Invest. 1993; 68:109-107.9. Williams ES. Canine Distemper. In: Williams ES, Barker IK, eds. Infectious diseases of wild mammals. 3rd ed. Ames, IA: Iowa State Press; 2001:50-59.
10. Qiu W[1], Zheng Y, Zhang S, Fan Q, Liu H, Zhang F, Wang W, Liao G, Hu R. Canine distemper outbreak in rhesus monkeys, China. Emerg Infect Dis. 2011 Aug;17(8):1541-3.
11. Sakai K[1], Nagata N, Ami Y, Seki F, Suzaki Y, Lethal canine distemper virus outbreak in cynomolgus monkeys in Japan in 2008. J Virol. 2013 Jan;87(2):1105-14.

CASE IV: 09-1045 (JPC 3164901).

Signalment: 5 year old, ovariohysterectomized female Cavalier King Charles spaniel, *Canis familiaris*.

History: An adult spayed female Cavalier King Charles Spaniel reported to be 5 years old from a the household with multiple dogs exhibiting increased respiratory rate and cough. During thoracic radiographs the patient became agonal and arrested despite attempted cardiopulmonary resuscitation. Radiographs revealed pneumonia. The patient was presented for necropsy 1.5 hours following death

Gross Pathology: The trachea is diffusely mildly compressed dorsoventrally. Excluding a limited regional portion of the cranial aspect of the left cranial lung lobe, the lungs are diffusely dark red, heavy, and sink in formalin. The heart is mildly

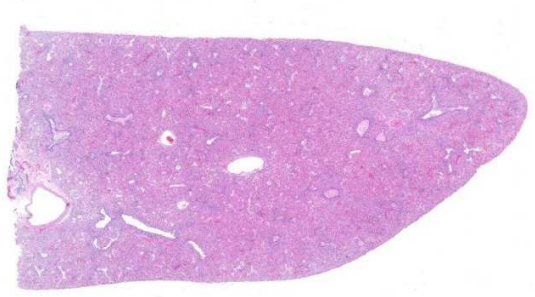

Lung: At subgross magnification, the lung is markedly congested, diffusely hypercellular, and there are blood vessels are surrounded by perivascular cuffs. (Photo courtesy of: University of Tennessee College of Veterinary Medicine, Department of Pathobiology, 2407 River Drive, Room A201, Knoxville, TN 37996 http://www.vet.utk.edu/)

enlarged with mild nodular thickening of the mitral valve. A small portion of the cerebellar vermis protrudes through a mildly narrowed and irregular foramen magnum.

Laboratory results:

Microbiology
Sample: Lung
Test: Aerobic Culture
Result: No growth seen in 3 days

PCR/DNA sequencing
99 % nucleotide identity with *Lycoperdon pyriforme* (AY854075.1, strain AFTOL-ID-48) over 682 bp.

Histopathologic Description: Lung: Alveoli and bronchioles frequently are filled with macrophages, neutrophils, cellular debris, erythrocytes, multinucleate giant cells and edema. The macrophages are frequently vesciulate, occasionally glassy eosinophilic material (hyalin membranes). Alveolar epithelial cells are multifocally cuboidal (type II pneumocyte hyperplasia) with rare binucleate and multinucleate cells. There is multifocal loss of the bronchiolar epithelium, with infrequent epithelial dysplasia. A few peribronchiolar macrophages contain black granular pigment (anthracosis). Moderate numbers of plasma cells with fewer lymphocytes surround pulmonary vessels. Vascular endothelial cells are frequently hypertrophic. Pleural mesothelial cells are hypertrophic.

Contributor's Morphologic Diagnosis: Marked, diffuse, histiocytic interstitial pneumonia with fungal spores.

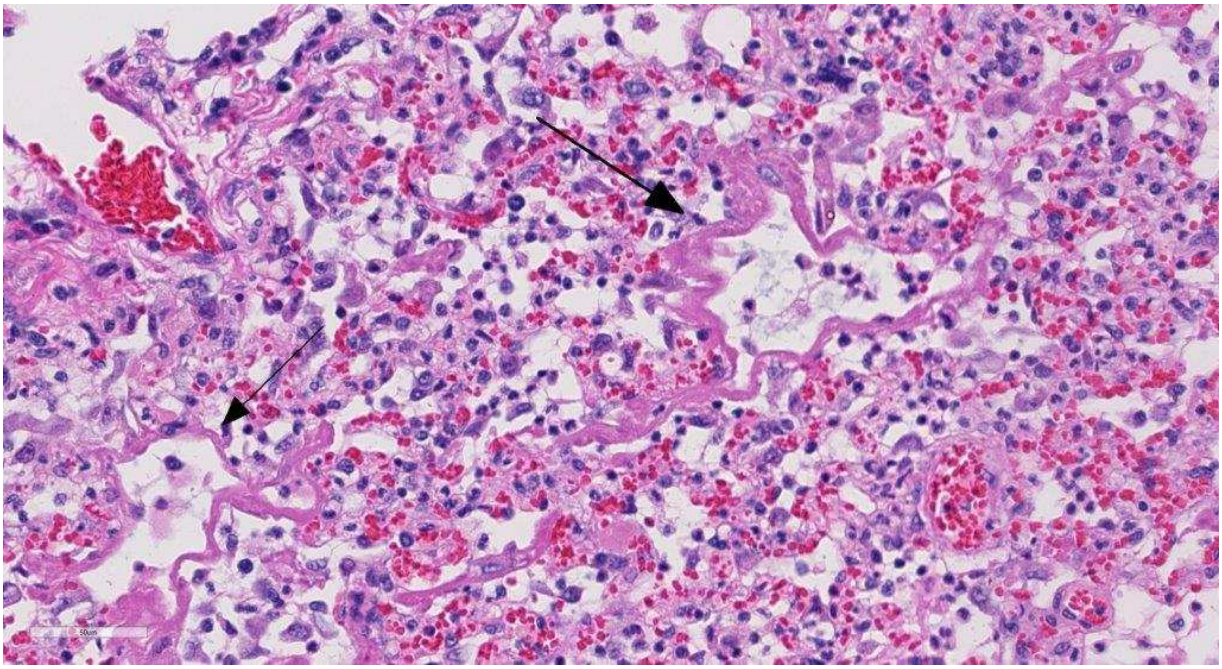

Lung, dog. Alveoli and distal airways are often lined by thick mats of fibrin (hyaline membranes). Alveoli contain moderate numbers of neutrophils and macrophages as well as fibrin. Septa are expanded by edema, fibrin, as well as increased numbers of circulating neutrophils. (HE, 260X)

containing cellular and karyorrhectic debris. Random, individual to multiple, golden-brown, 3-5µm diameter fungal spores are present both within macrophages and free within the alveolar lumens. Alveolar septa are occasionally lined by finely fibrillar to

Contributor's Comment: The intra-histiocytic and free fungal spores within the lung were identified as spores of "puffball" mushrooms by PCR and DNA sequencing. Eleven species of puffball mushrooms

(*Lycoperdon sp*.) are indigenous to the area from which this case originated (greater Smoky Mountains). Inhalation of spores has been reported infrequently in association with pneumonia (pulmonary lycoperdonosis) in dogs[1,8] and humans[7,9].

JPC Diagnosis: Lung: Pneumonia, interstitial, necrotizing, fibrinosuppurative, and histiocytic, diffuse, chronic, severe with hyaline membrane formation and rare intrahistiocytic fungal spores.

Conference Comment: Pulmonary lesions caused by the inhalation of *Lycoperdon sp.* spores are theorized to result from the host hypersensitivity response to fungal spores acting as foreign bodies rather than an infectious process.[2,7] The failure to culture *Lycoperdon* from a reported case and inability of this saprophytic fungus to germinate under normal physiologic body temperatures supports this theory.[7] Hypersensitivity pneumonitis (HP), also known as extrinsic allergic alveolitis, is caused by

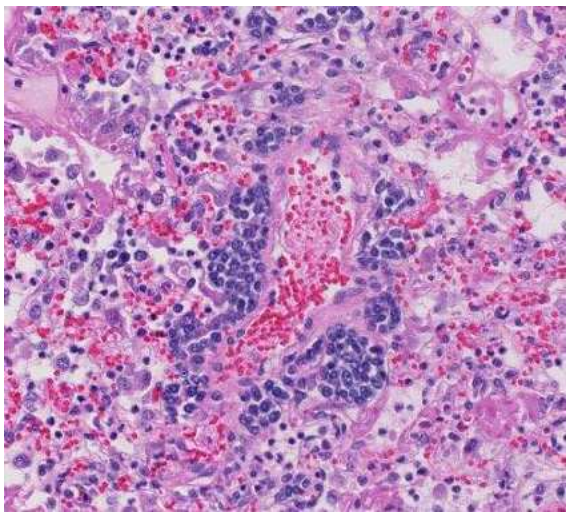

Lung, dog. Vessels throughout the sections are cuffed y 3-5 layers of lymphocytes and fewer plasma cells. (HE, 280X)

intense and often prolonged exposure to inhaled organic antigens such as fungal spores, but can also include bacterial products and animal proteins. This disease is commonly diagnosed in dairy cows and horses housed indoors and usually affect multiple animals within a group. It results from chronic inhalation of spores of thermophilic actinomycetes (*Saccharopolyspora rectivirgula*) found in moldy hay.[5,6] This is followed by an antibody response to inhaled antigen and local deposition of antigen-antibody complexes (Arthus reaction) as well as the formation of multifocal granulomas suggesting a T-cell-mediated response. This type of reaction suggests both type III and type IV hypersensitivity response [2,5,7] (See WSC 2012-2013, conference 22, case 4 for a review of hypersensitivity reactions).

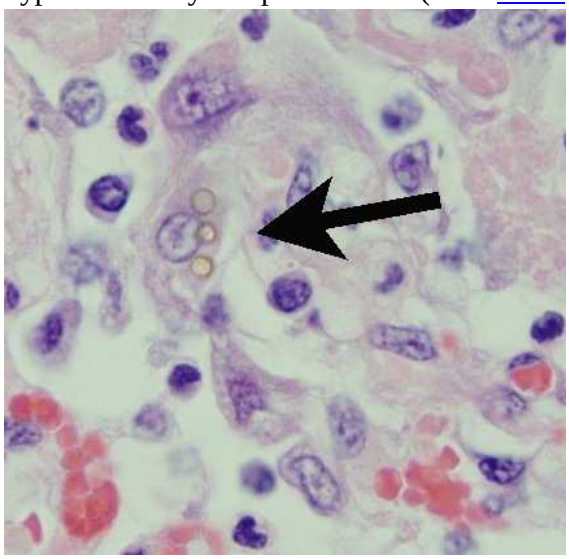

Lung: Rare macrophages contain single or multiple 4-6um golden-brown fungal spores. (HE, 400X)(Photo courtesy of: University of Tennessee College of Veterinary Medicine, Department of Pathobiology, 2407 River Drive, Room A201, Knoxville, TN 37996 http://www.vet.utk.edu/)

Characteristic lesions in animal and human HP include proliferation of type II pneumocytes and fibrosis of alveolar septa and peribronchiolar tissue. In severe cases, hyaline membranes composed of fibrin, serum proteins, and cell debris line the alveolar septa.[5] This hyaline membrane

causes alveolar occlusion resulting in severe hypoxia and death.

Conference participants noted the severe necrotizing and inflammatory changes to the lung interstitium, but had difficult time finding the rare fungal spores present in the tissue. Interestingly, clinical disease of lycoperdonosis in humans and dogs only occurs following a massive inhalation dose of puffball conidia[7]; however in this section there is a paucity of spores present. As a result, there was discussion of differentials

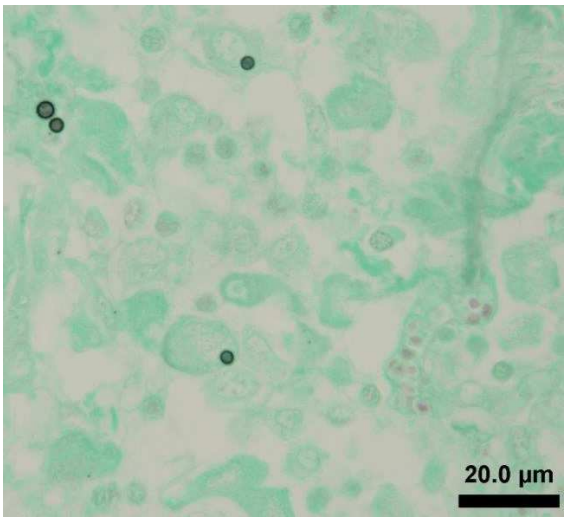

Lung: Fungal spores are argyrophilic on a Gomori methenamine silver stain. (GMS, 400X) (Photo courtesy of: University of Tennessee College of Veterinary Medicine, Department of Pathobiology, 2407 River Drive, Room A201, Knoxville, TN 37996 http://www.vet.utk.edu/)

for hyaline membrane formation, which is the most striking histologic feature in this case. Acute respiratory distress syndrome (ARDS) in the dog was discussed as having a similar histopathologic appearance to this case. In addition to hyaline membranes, type II pneumocyte hyperplasia, and bronchiolar epithelial necrosis is a consistent feature of ARDS. Inciting causes include: trauma, shock, disseminated intravascular coagulation, septicemia, smoke inhalation, oxygen toxicity, viral infection, and strangulation among others.[4]

This case was additionally studied in consultation with the Department of Pulmonary and Mediastinal Pathology at the Joint Pathology Center, who disagreed with the purported mechanisms discussed above, based on the morphologic changes noted in this section. Their interpretation is that this section of lung is diagnostic for diffuse alveolar damage (DAD) due to a toxic reaction to *Lycoperdon* spores rather than HP, published in a case report from this animal.[2] DAD is the most commonly identified form of interstitial lung disease and is the histologic correlate to the clinical condition of ARDS, discussed by conference participants.[4] The pulmonary pathologists describe an intra-alveolar inflammatory infiltrate composed predominantly of neutrophils and macrophages. This is admixed with focal plasma cells and lymphocytes, hyaline membranes, and acute inflammation of bronchiolar epithelium, along with multifocal fungal spores. They see no histologic evidence to support the diagnosis of HP. They also note the importance of recognizing this entity as DAD, and not HP, due to the high mortality rate for DAD, even with intensive supportive treatment.

Contributing Institution: University of Tennessee
College of Veterinary Medicine
Department of Pathobiology
www.vet.utk.edu/departments/path

References:

1. Aleghat T, Kellett-Gregory L, Van Winkle T: Lycoperdonosis in a dog, *Vet Pathol*. 2009;46:1046.
2. Alenghat T, Pillitteri C et al. Lycoperdonosis in two dogs. *J Vet Diagn Invest*. 2010;22:1002-1005.

3. Buckeridge D, Torrance A, Daly M. Puffball mushroom toxicosis (lycoperdonosis) in a two-year-old dachshund. *Vet Rec.* 2011;168:304.
4. Caswell J, Williams K. Respiratory system. In: Maxie MG, ed. *Jubb, Kennedy, and Palmer's Pathology of Domestic Animals*. Vol 2. 6th ed. Philadelphia, PA: Elsevier Saunders; 2016: 514.
5. Husain AN. The Lung. In: Kumar V, Abbas AK, Aster JC, eds. *Pathologic Basis of Disease.* 9th ed. Philadelphia, PA: Elsevier Saunders; 2015:694-695.
6. Lopez A. Respiratory system, mediastinum, and pleurae. In: Zachary JF, McGavin MD, eds. *Pathologic Basis of Veterinary Disease.* 5th ed. St. Louis, MO: Elsevier; 2012:513.
7. Munson E, Panko D, Fink, J. Lycoperdonosis: Report of Two Cases and Discussion of the Disease: *Clin Microbiol Newsl*. 1997;19(3):17-20.
8. Rubensohn M: Inhalation pneumonitis in a dog from spores of puffball mushrooms. *Can Vet Journal*. 2009;50(1):93.
9. Taft T, Cardillo R et al. Respiratory illness associated with inhalation of mushroom spores-Wisconsin, 1994. *MMWR Morb Mortal Wkly Rep*. 1994;43(29):525-526.